We are IntechOpen, the world's leading publisher of Open Access books Built by scientists, for scientists

4,800
Open access books available

122,000
International authors and editors

135M
Downloads

Our authors are among the

154
Countries delivered to

TOP 1%
most cited scientists

12.2%
Contributors from top 500 universities

CLARIVATE ANALYTICS BOOK CITATION INDEX INDEXED

WEB OF SCIENCE™

Selection of our books indexed in the Book Citation Index in Web of Science™ Core Collection (BKCI)

Interested in publishing with us?
Contact book.department@intechopen.com

Numbers displayed above are based on latest data collected.
For more information visit www.intechopen.com

Chapter 5

An Experimental Crack Propagation Analysis of Aluminum Matrix Functionally Graded Material

Arzum Ulukoy, Muzaffer Topcu and Suleyman Tasgetiren

Additional information is available at the end of the chapter

http://dx.doi.org/10.5772/62428

Abstract

In this study, a functionally graded cylindrical specimen was obtained via centrifugal casting and its fatigue crack behavior was investigated. Aluminum 2014 alloy and SiC were used as matrix material and ceramic particle, respectively. The distribution of SiC and the mechanical properties of material through cylinder wall thickness were varied because of the centrifugal force during centrifugal casting. Variations in microstructure and hardness were examined. A cylindrical specimen was cut through its thickness in four sections through vertical slicing. Tensile strength was tested on each section to determine the mechanical properties that can be varied such as Young's modulus, tensile strength, and yielding stress. To investigate the effect of variation in the mechanical properties and distribution of SiC particles on fatigue crack behavior, fatigue crack growth tests were applied under tensile cyclic load with stress ratio $R = 0.1$. The samples were prepared in three separate groups: central notched, single-edge notched on SiC-rich side, and single-edge notched on aluminum-rich side. It was found that SiC distribution affected fatigue crack initiation and propagation. The fatigue life increased up to 350% because of increasing SiC ratio for central notched specimens. Cracks were started out later on the single-edge notched SiC-rich side compared to aluminum-rich side whose fatigue life increased up to 500%. In addition, it was found that unreinforced aluminum material's fatigue life was lower than that of reinforced material.

Keywords: Functionally graded material, Aluminum matrix, Franc2D, Crack propagation, Fatigue

1. Introduction

Material is used to perform a design. The design engineer expects some material properties, either single or combinations of one or more properties, from materials for engineering design such as light weight, strength, fatigue strength, high temperature strength, high fracture

toughness, corrosion resistance, wear resistance, electrical properties, and manufacturability [1, 2]. Although the metallic materials have higher fracture toughness and better thermal shock resistance than the ceramics, their high temperature resistance is lower than of the ceramics. Ceramic materials have low density, good high temperature resistance, and good creep resistance, but their thermal shock resistance is low [2–5]. Man-made polymer materials have been used for the past 100 years because they are lightweight, cheap, highly resistant to corrosion, and wear resistant. Also, the production of polymer materials is much easier than the metallic and ceramic materials. However, their low mechanical strength limits their use in structural design [2]. Composite materials are obtained by combining ceramic, metallic, and/or polymer materials. Thus, the designer can benefit from the superior properties of two different materials simultaneously [2, 4].

Metal matrix composites (MMCs) reinforced with ceramic particles provide the required material properties in many engineering applications. High strength, high corrosion resistance, and stiffness of MMCs have made them suitable for their use in, particularly, aerospace, aviation, automobile, and mineral processing industry [6, 7]. Particulate reinforced MMC materials are cheaper and have higher abrasion resistance and higher temperature stability than that of materials, and they are being used widely in many areas compared to the continuous fiber reinforced composites [6, 7].

Functionally graded materials (FGMs) can be considered as a subcategory of composite materials. The microstructure, mechanical, and thermal properties are changed throughout the thickness or width of the material depending on a function [8–10].

The function type and consequently FGMs' properties are primarily related to mechanical/thermal properties and compatibility of matrix and reinforced materials, FGM thickness or width, and manufacturing method. Function can occur in three different ways depending on the following factors: exponentially, linearly, and according to the rule of force. The mechanical/thermal properties of material such as Young's modulus, yielding stress, tensile stress, fatigue, and thermal/electrical conductivity properties can vary depending on the function type [4, 8–12].

There are some basic manufacturing methods for graded materials, which include powder metallurgy, physical vapor deposition (PVD), chemical vapor deposition (CVD), plasma spray, thermal spray, combustion synthesis (SHS), centrifugal casting, and polymerization [4, 10, 12–29]. Recently developed methods are also available: modified stir casting, centrifugal sintering, gradient slurry disintegration and deposition, and powder cold spray before cold isostatic sintering [30–33].

MMCs reinforced with ceramic particles have been used for a long time because they can be easily manufactured. MMCs are inexpensive than the other composite types and have improvable thermal and mechanical properties [7]. When two different types of materials are combined, it can lead to formation of additional thermal and residual stresses. It is known that discontinuities and thermal stress can be decreased on ceramic–metal interface using FGMs [4, 8, 9].

http://dx.doi.org/10.5772/62428

Crack propagation that causes sudden or stepped fracture occurs when stress concentration at the tip of crack overcomes strength of material [34]. For a linear elastic material, stress concentration at the tip can be represented by K_I, K_{II}, and K_{III}, which are stress intensity factors in opening, sliding, and tearing conditions, respectively. Critical value of stress intensity factor Kc must be equal to K_I for crack propagation under Mode I load.

There are many analytical and numerical studies on fatigue and fracture mechanics of FGMs [34–51]. Theoretical crack propagation analyses of FGMs indicate that the crack tip stress is different from that of the homogeneous material [34, 38–40]. The studies on the subject demonstrate that grading direction and function affect the crack propagation. It is found that FGMs have shown better performance at increasing crack growth compared with homogeneous materials.

Under asymmetric loadings, the crack propagates perpendicularly to grading direction, which changes the direction of crack [43]. However, under symmetric loadings, the crack propagates in parallel to grading direction [42]. Crack propagation experiments in grading materials have been carried out using the following: direction of crack propagation (in parallel to grading direction) under different loading cycles (regularly increasing or decreasing loading [53–54], periodic mechanical loading [50–52], and periodical thermal loading [58–59]). In the experiments where crack propagation was perpendicular to the grading direction, fracture happened quickly [60–62]. Therefore, the effect of grading on the stress concentration factor could not be calculated. Compared to homogeneous material, FGMs' fracture behavior is altered by FGM composition and properties by four of the following [63]:

1. Variable stress region: Crack direction in FGMs is changed by graded mechanical properties (Young's modulus, E, and the Poisson ratio, υ), but not in homogeneous materials. As a result, fracture loads and crack path are affected by grading material properties.

2. Crack tip toughness: Since the chemical composition of material changes, internal fracture toughness (K_0) becomes a function ($K_0(a)$) that changes according to the position of the grading.

3. Hardening rate of the crack opening: Change in the microstructure and the chemical composition of graded region changes the characteristics of hardening of the crack opening too. Crack closure as in homogeneous materials depends on not only being on the back of the crack but also the position of the cracks in graded region.

4. Residual and thermal stresses: Thermal and residual stresses in FGMs effect fracture behavior and crack tip stress zone [53–66].

In Equation (1), σ_{ij} represents the crack tip stress, K_α (α = I, II, III) stress intensity factors, θ the angle with respect to the plane of the crack, r the distance from crack tip, δ the Kronecker delta, σ_T the transverse stress, $f_{ij}^{(\alpha)}(\theta)$ angular functions, and $1/\sqrt{r}$ the singularity of crack tip stress. Studies by Delale and Erdogan [35] and Eischen [39] showed that the singularity of crack tip stress of continuous or partially graded materials is similar to that of homogeneous materials.

Jin and Noda [41] verified this situation by determining that the angular distribution function of the elastic and plastic crack tip area ($f_{ij}(\theta)$) is the same.

$$\sigma_{ij} = \frac{K_\alpha}{\sqrt{2\pi r}} f_{ij}^{(\alpha)}(\theta) + \delta_{1i}\delta_{1j}\sigma_T + A_\alpha \sqrt{2\pi r} w_{ij}^{(\alpha)}(\theta) \tag{1}$$

Also, the studies conducted by Eischen [39] and Jin and Noda [41] have shown that FGMs crack tip stress (σ_{ij}) and displacement (u_i) (Eq. (2)) are the same form as homogeneous material. In Equation (2), K_α (α = I, II) represents stress intensity factors, r the distance from crack tip, θ the angle with respect to the plane of the crack, $g_i^{(\alpha)}(\theta)$ angular functions, E_{tip} the Young's modulus at crack tip, and υ_{tip} the Poisson ratio at crack tip. These results mean that the stress intensity factor is a determinative fracture parameter for FGMs just like in homogeneous material [67]. Similar results have been found for dynamically propagated cracks by Parameswaran and Shukla [68].

$$u_i \approx \frac{K_\alpha\left(2 + 2\upsilon_{\text{tip}}\right)}{E_{\text{tip}}}\sqrt{\frac{8r}{\pi}} g_i^{(\alpha)}(\theta) \tag{2}$$

Continuous or stepped grading prevents the abnormal stress behavior of cracks when the interface of two materials is combined [69]. Moreover, Delale and Erdogan [35] found that the effect of spatial variation of the Poisson ratio on the stress singularity can be neglected.

Fracture behavior depending on orientation in the grading region can be defined by considering two limit states [63]:

1. Crack propagation is parallel to grading direction: crack does not digress although effective fracture toughness changes.
2. Crack propagation is perpendicular to grading direction: asymmetric crack tip zone causes crack to deflect.

In the cracks that are parallel to the direction, stress at the crack tip region becomes symmetric and it is expected that crack opens toward the grading direction. FGM crack tip stresses in graded regions are significantly lower than in materials with combinations of two material properties [37, 70, 71]. Stress intensity factor of FGMs is found to be greater than that of homogeneous materials. Material grading profile and position of the crack effect stress intensity factor too. When grading step increases, its value increases [35, 37, 42, 72]. Grading format also effects the stress intensity factor. If exponential value n is bigger than 1 ($n > 1$), the stress intensity factor is in tendency to decrease compared to $n < 1$ situation [70–72]. Spatial composition changes, which have an important effect on effective fracture toughness of the FGM composites, can effect thermal stress distribution throughout its width. Growing fracture toughness depends on residual stresses partially [53, 64, 73]. As residual stresses change by

http://dx.doi.org/10.5772/62428

composition of FGM, compressive stresses increase the resistance of crack against growing fracture [64].

Critical value of stress intensity factor K_c must be equal to K_I for crack propagation under crack opening mode. In the ongoing process, crack growth rates da/dN in every period can be found by using Paris Equation (Eq. (3)), where N is the number of cycles to failure, c and m are material constants [34].

$$\frac{da}{dN} = c\Delta K^m \tag{3}$$

Studies related to FGMs' fatigue and fatigue fracture behaviors have been conducted using numerical and analytical methods and new approaches are developed to date. However, there are hardly enough experimental studies to support this.

In this study, aluminum 2014 matrix reinforced with SiC FGM was manufactured via centrifugal casting. The effect of SiC distribution on the mechanical and fatigue fracture properties was determined and analyzed experimentally.

2. Experimental results and analysis

Two functionally graded aluminum 2014 alloy (1.18% Si, 4.9% Cu, 1.04% Mn, in wt.) matrix materials reinforced with 20% in wt. and 9 μm SiC particles were produced by centrifugal casting. Density of SiC particles is higher than that of aluminum, 3.2 gr/cm^3 and 2.8 gr/cm^3, respectively. As a result of the centrifugal force effect, the distribution of SiC particles was varied through the wall thickness of the cylinder. More SiC particles were dispersed to the outer diameter of the FGM cylinder under these circumstances, as expected. By changing casting wall thicknesses, two cylinders having different mechanical properties were produced. The specimens were named FGM1 and FGM2, and SiC-rich and aluminum-rich regions were formed on both of FGM1 and FGM2. FGM1's wall thickness was higher than FGM2's. This result is compatible with the previous studies on the subject [74–83]. Taking into account the wear, fatigue, and fretting behaviors of FGM from previous studies, an aging process was performed (solutionizing at 500 °C, followed by water quenching and reheating for aging at 145 °C for 10 h, followed by water cooling) [75, 82, 83].

Tensile tests were performed using specimens sliced through the wall thickness and were numbered from 1 to 5 for FGM1 and FGM2 according to their position in the cylinder (from the innermost to the outermost layer). Tensile strength was tested on each section to determine the mechanical properties that can be varied such as Young's modulus (E), tensile strength (R), and yielding stress (R_e) (Figures 1–3). Tensile experiments were conducted using video extensometer at 1 mm/min tensile speed. Obtaining tensile specimens from the cylindrical FGM is shown in Figure 4.

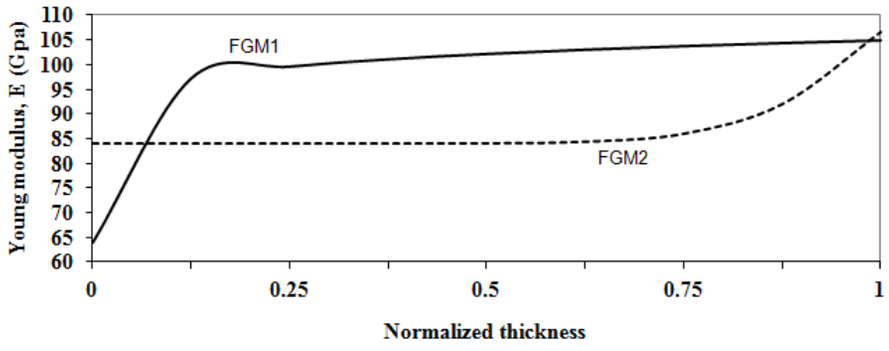

Figure 1. Young's modulus variations of FGM1 and FGM2 [84].

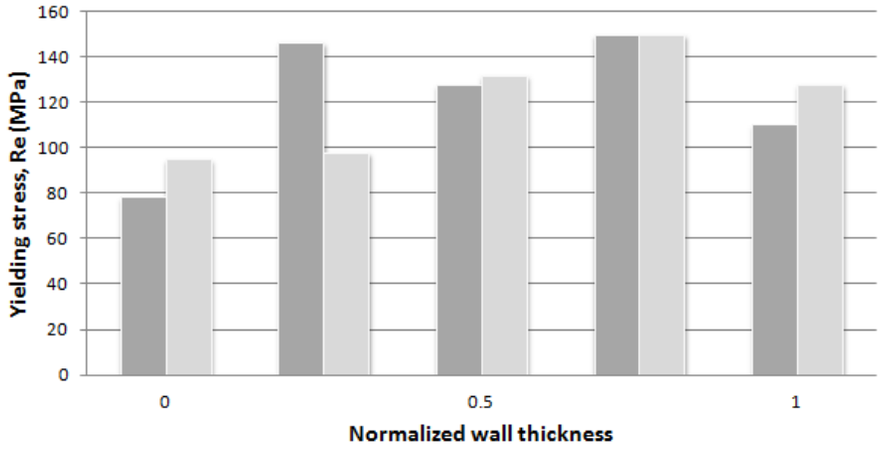

Figure 2. Yielding stress variations of FGM1 and FGM2.

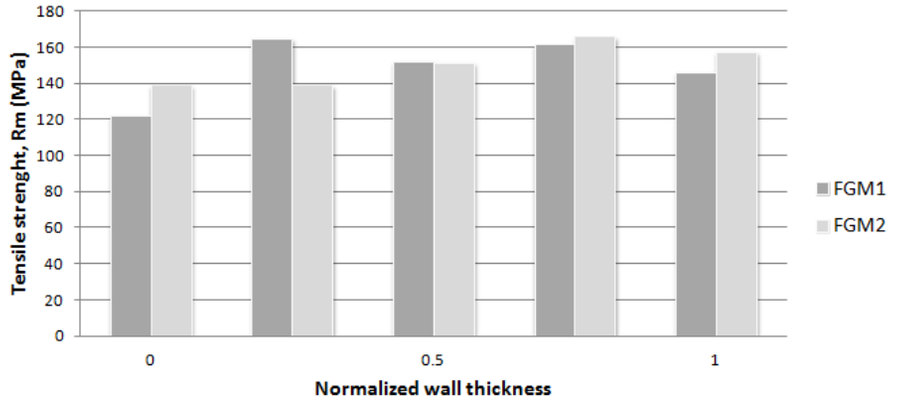

Figure 3. Tensile strength variations of FGM1 and FGM2.

http://dx.doi.org/10.5772/62428

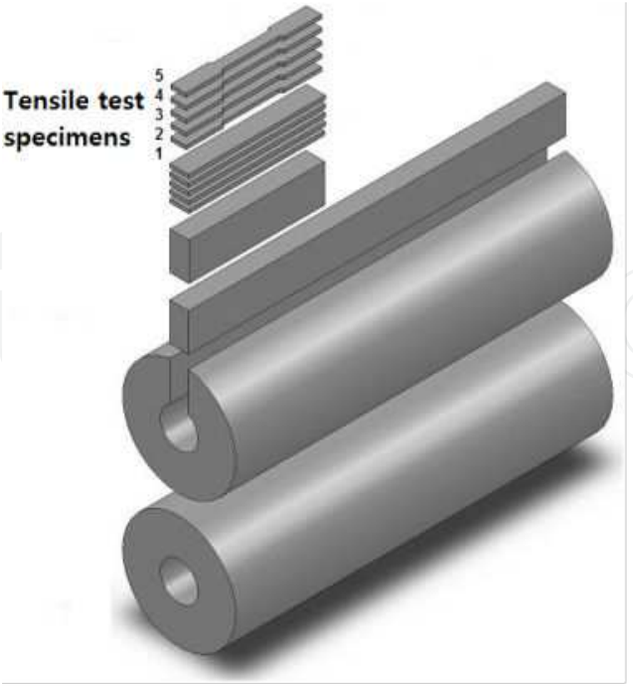

Figure 4. Obtaining tensile test samples from cylindrical FGM.

Due to the higher density of SiC particles (relative to aluminum 2014), many more particles were dispersed to the outer diameter of FGM cylinder during centrifugal casting. This produced a gradient in the Young's modulus, from the inside to the outside layer of cylinder (Figure 1) [84]. It was observed that SiC distribution under centrifugal force and wall thickness of cylinders effected Young's modulus variation. As wall thickness of cylinder decreased, it was observed that Young's modulus value (innermost of cylinder) increased from 65 MPa to 84 MPa. Grading functions of FGMs were differed from each other due to the distribution of SiC. Young's modulus values of the outermost region of cylinders were similar (105–106 MPa). It was observed that wall thickness of FGM and manufacturing process had an impact on the composition and mechanical properties of FGM.

As mentioned above, FGMs' properties can vary exponentially, linearly, and according to the rule of force. In this study, Young's modulus variation was calculated according to the rule of force to compare with experimental results using Equations (4) and (5). In these equations, $E(x)$ represents Young's modulus at x point, E_1 base material Young's modulus, E_2 reinforcing material Young's modulus, t the width/thickness of FGM, x the distance from the starting point, $g(x)$ the distance function, and p the gradient exponent. The gradient exponent (p) was calculated using equations as 0.1 and 7 for FGM1 and FGM2, respectively.

$$g(x) = \left(\frac{x}{t}\right)^p \tag{4}$$

$$E(x) = E_1\left(1 - g(x)\right) + E_2 g(x) \tag{5}$$

Tensile and fatigue crack growth tests were performed with a 5-ton capacity Instron fatigue servo-hydraulic test device. Two cylindrical specimens were cut through their wall thickness in four sections via vertical slicing as shown in Figure 4. Tensile tests were carried out to determine the crack opening properties using video extensometer at 1 mm/min tensile speed.

To investigate the effect of variation in mechanical properties and distribution of SiC particles on fatigue crack behavior, fatigue crack growth tests were applied under tensile cyclic load with stress ratio $R = 0.1$. The samples were prepared according to the ASTM E647 (2011) [85] in three separate groups: central notched (middle tension, M(T)), single-edge notched (SE(T)) on SiC-rich side, and single-edge notched (SE(T)) on aluminum-rich side (Figure 5). The test specimens' dimensions are shown in Figure 6. M(T) and (SE(T)) samples are prepared according to the ASTM E647 (2011) [85]. Samples were processed by laser cutting method. According to the ASTM E647 (2011) [85] standard, crack length to be opened must be at least $0.2W$; sample length $L > 0.3$. W represents width belonging to the sample. Notch length opened on M(T) specimens $2a = 13$ mm, notch length opened on SE(T) $a = 5.5$ mm [86]. Both tensile and fatigue experiments were applied to these samples. Two digital portable microscopes, as shown in Figure 7, were used to determine the crack beginning from notch tip and propagation of that crack. Applied maximum load determined with respect of minimum yielding stress after tensile tests were applied to central and single-edge notched specimens (Eq. (6)).

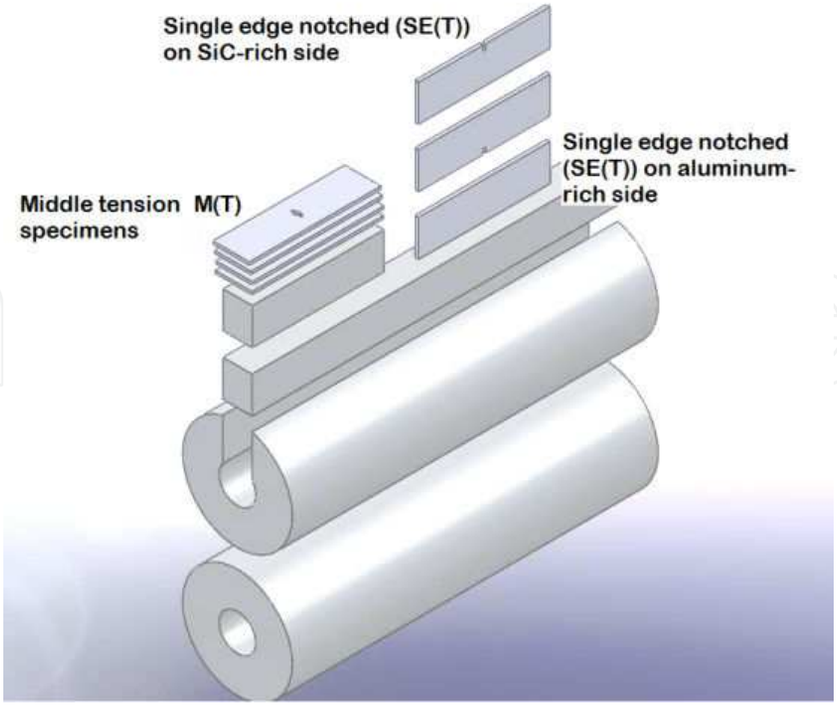

Figure 5. Obtaining fatigue crack growth test samples from cylindrical FGM [84].

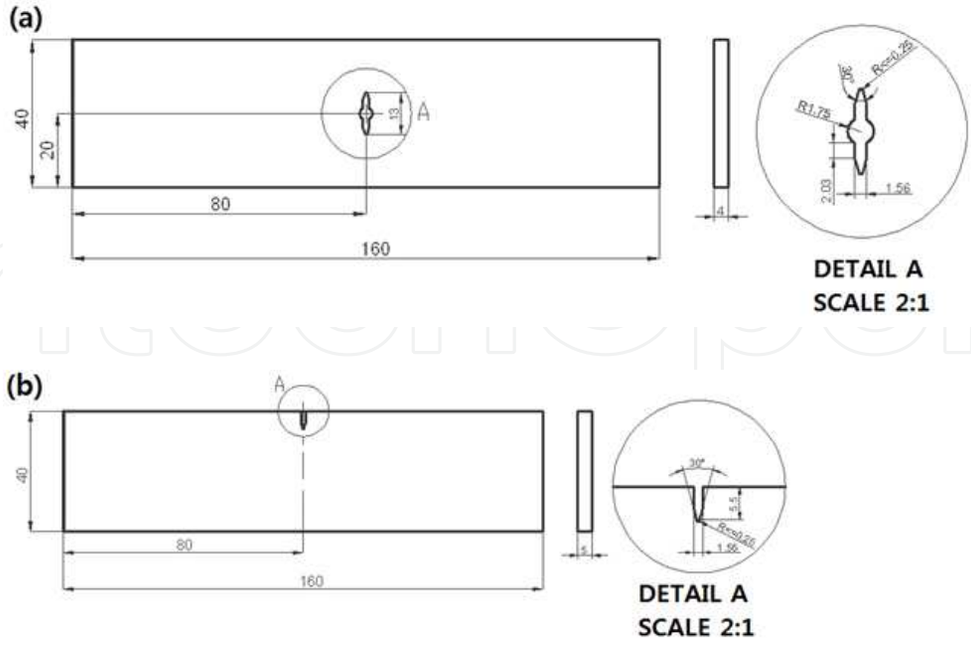

Figure 6. Dimension of fatigue crack growth test samples: (a) middle tension M(T)), (b) single-edge notched (SE(T)) [84].

$$\sigma_{max} = 0.3Re_{min} \tag{6}$$

Stress ratio (R) is important for calculations of load increment (ΔP) and stress concentration factor increment (ΔK) for homogeneous material according to the ASTM E647 (2011) (Eq. (7–9)) [85].

$$R > 0 \Rightarrow \Delta P = P_{max} - P_{min} \tag{7}$$

$$\begin{aligned} &R \le 0 \Rightarrow \Delta P = P_{max} \\ &2a/W < 0.95 \Rightarrow \Delta K = \frac{\Delta P}{B}\sqrt{\frac{\pi\alpha}{2W}}\sec\frac{\pi\alpha}{2} \end{aligned} \tag{8}$$

$$R = \frac{P_{min}}{P_{max}} = \frac{\sigma_{min}}{\sigma_{max}} = \frac{K_{min}}{K_{max}} \tag{9}$$

For $2a/W < 0.95$ situation, M(T) specimens were accepted homogeneous and Equations (5) and (6) were used in calculations. a represents crack half-length. If $2a/W$ is greater than or equal to 0.95, it is accepted that crack will be instable and then probably fracture will be occur. The

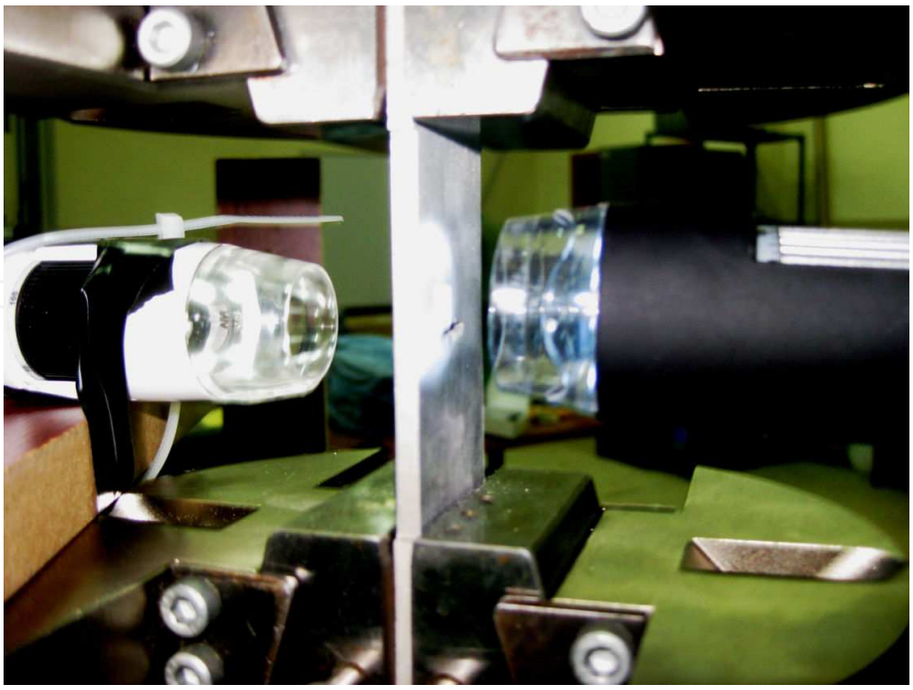

Figure 7. The digital microscopes used in experiments

stress ratio $R = 0.1$ and frequency $f = 5$ Hz were selected as fatigue crack growth experiment parameters. SE(T) specimens' notch was parallel to the grading direction.

Load-crack tip opening diagrams of M(T) specimens obtained from FGM1 after tensile tests are shown in Figure 8. Here, 1–4 refer to specimen numbers from innermost (aluminum-rich side) to outermost (SiC-rich side) regions of cylinder. It can be understood that Al-rich side fractured at a lower load value. Since SiC rate increased, load carrying capacity of specimens increased. SiC-rich side fractured at a higher load value than the others.

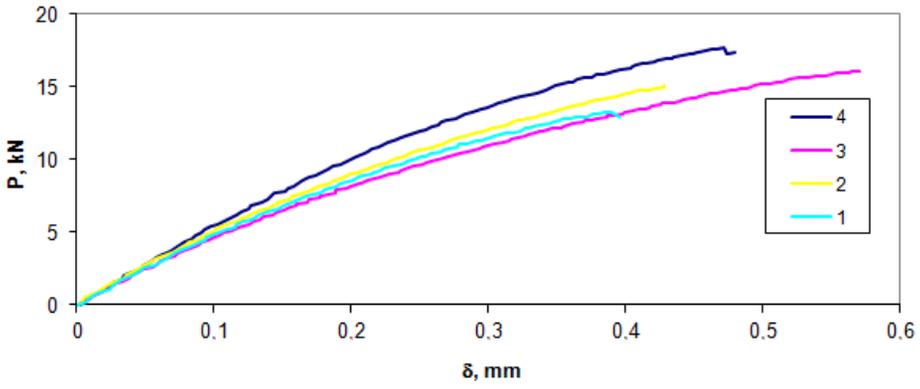

Figure 8. Load-crack tip opening diagrams of M(T) specimens obtained from FGM1.

Load-crack tip opening diagrams of SE(T) specimens obtained from FGM2 after tensile tests can be seen in Figure 9. The specimen (SE(T)) on SiC-rich side was fractured at a higher load

http://dx.doi.org/10.5772/62428

than the (SE(T)) on aluminum-rich side specimen. Curves are almost continued in the same way until opening value is 0.5 mm. However, it is seen that (SE(T)) on aluminum-rich side specimen fractured when load value is up to 12 kN. On the other hand, (SE(T)) on SiC-rich side specimen continues to open till an 1.6 mm opening value at 20 kN load.

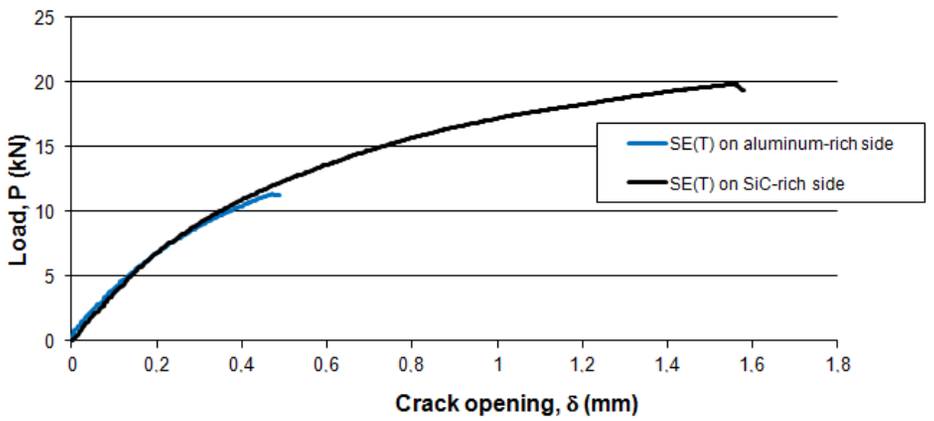

Figure 9. Load-crack tip opening diagrams of SE(T) specimens obtained from FGM2 [84].

Number of cyclic load-crack propagation diagram of M(T) samples obtained from FGM2 with stress ratio $R = 0.1$ condition is shown in Figure 10. Here, 1–4 refer to specimen numbers from innermost (aluminum-rich side) to outermost (SiC-rich side) regions of cylinder, and specimens fractured at 12,880, 27,000, 34,000, and 48,000 number of cyclic loads, respectively. It can be seen that the fatigue life increases to almost 350% because of increase in SiC rate.

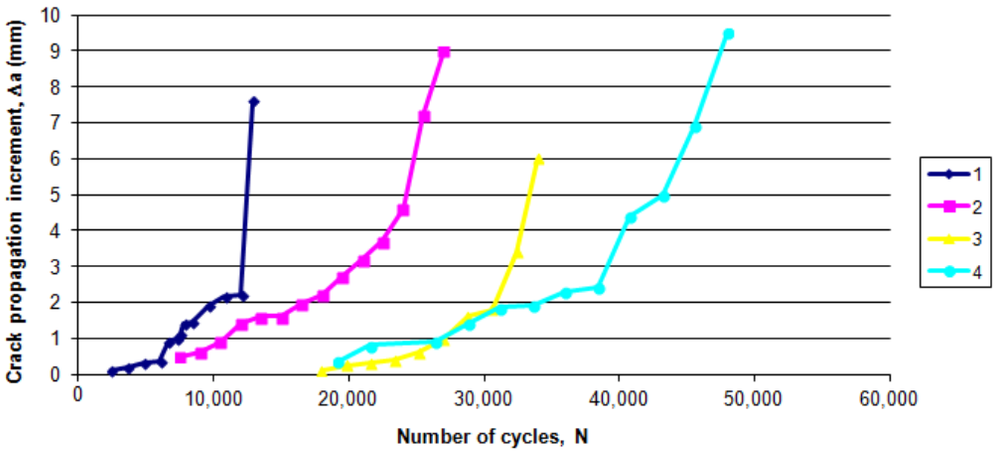

Figure 10. Number of cyclic load-crack propagation diagram of M(T) samples obtained from FGM2: 1–4 refers to specimen numbers from innermost (aluminum-rich side) to outermost (SiC-rich side) [84].

Number of cyclic load-crack propagation diagram of SE(T) samples obtained from FGM1 (both of SiC-rich side and aluminum-rich side) with stress ratio $R = 0.1$ is shown in Figure 11. It was determined that the crack growing rate increased after 14,400 cycles for the aluminum-rich side SE(T) sample. However, after 28,800 cycles, the crack growing rate increased dramatically and after 36,850 cycles, sample fractured in a short time. On the other hand, SiC-rich side SE(T) sample's crack growth rate was very slow up to 13,000 cycles under the same cyclic load and after 13,000 cycles, the growth rate increased gradually. Crack growth rate increased dramatically after 190,000 cycles and sample fractured in a short time after 214,000 cycles. Under the same fatigue load, it was determined that the SiC-rich side SE(T) sample had fatigue life more than 500% compared to the aluminum-rich side SE(T) sample.

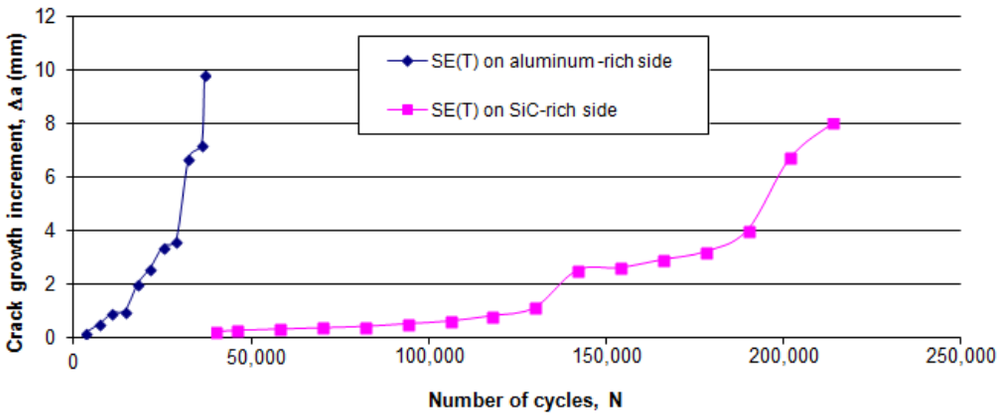

Figure 11. Number of cyclic load-crack propagation diagram of SE(T) samples obtained from FGM1 [84].

Number of cyclic load-crack propagation diagram of SE(T) samples obtained from FGM1 and FGM2 aluminum-rich side with stress ratio $R = 0.1$ condition is shown in Figure 12. A sample belonging to FGM2 displays a quick fracture behavior compared to FGM1. Whereas FGM2 sample fractured at 36,850cycles, FGM1 sample fractured at 238,000 cycles. FGM1's fatigue life was increased 1.5-fold compared to FGM2's fatigue life, which is explained by Young's modulus variation seen in Figure 1. Graphics show differences in variation of Young's modulus. SiC distribution in FGM2 increases from the innermost region to the outermost region till 0.2 times wall thickness, and then the rise slows down. In FGM1's inner region, distributions of SiC and in parallel with Young's modulus are higher than in the FGM2's. The Young's modulus determined as $E = 85$ GPa innermost of cylinder wall thickness does not visually increase by 0.75 times wall thickness.

After the fatigue crack growth experiments finished, c and m, which are material-dependent coefficients of the Paris-Erdogan equation (Eq. (3)), were found for each FGM2 M(T) specimens. The crack propagation behavior of the samples, which were from the inner diameter to the outside diameter of the cylinder numbered from 1 to 4, was observed differently in each of the samples. Therefore, the c and m coefficients were observed different from each other. The FGM's c and m coefficients are shown in Table 1.

http://dx.doi.org/10.5772/62428

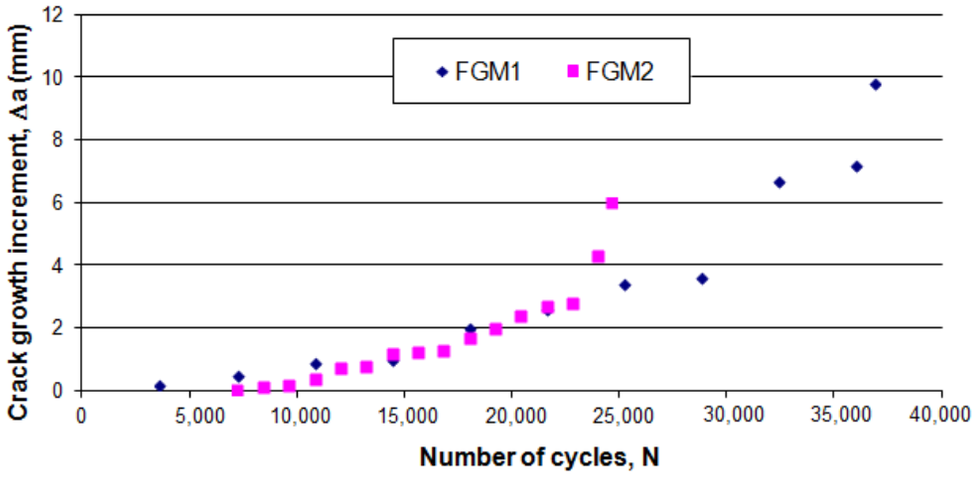

Figure 12. Number of cyclic load-crack propagation diagram of SE(T) samples obtained from FGM1 and FGM2 aluminum-rich side [84].

FRANC2D finite elements program have been developed by the fracture group of Cornell University [87]. The program is usually used for fracture mechanics and fatigue analysis. In this study, FRANC2D analysis was done for FGM2 M(T) specimens. The finite element model can be seen in Figure 13. It was accepted that the M(T) specimen was homogeneous in itself while modeling in FRANC2D. According to the analysis, obtained results from experimental and finite element modeling were similar to each other as seen in Figure 14.

	1	2	3	4
c	10^{-8}	10^{-8}	2×10^{-9}	6×10^{-9}
m	1.3632	1.0801	1.6678	1.2058

Table 1. Calculated *c* and *m* coefficients of FGM2 M(T) specimens: 1–4 refer to specimen numbers from innermost (aluminum-rich side) to outermost (SiC-rich side) regions of cylinder

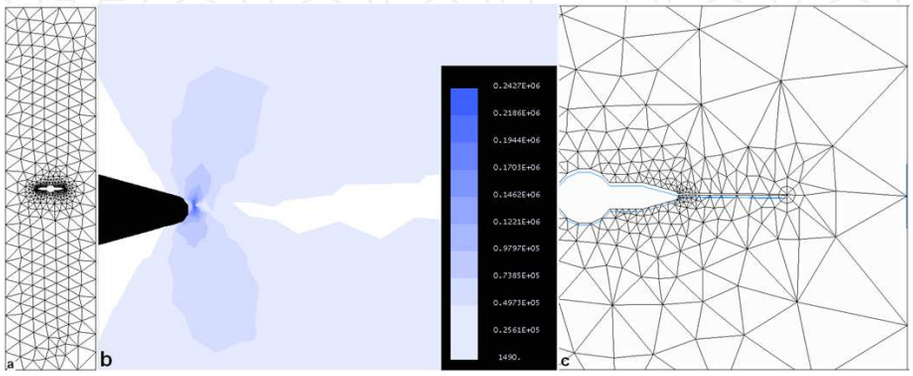

Figure 13. M(T) specimen modeling using FRANC2D program: (a) model, (b) maximum shear stress at crack tip, (c) deformation shape.

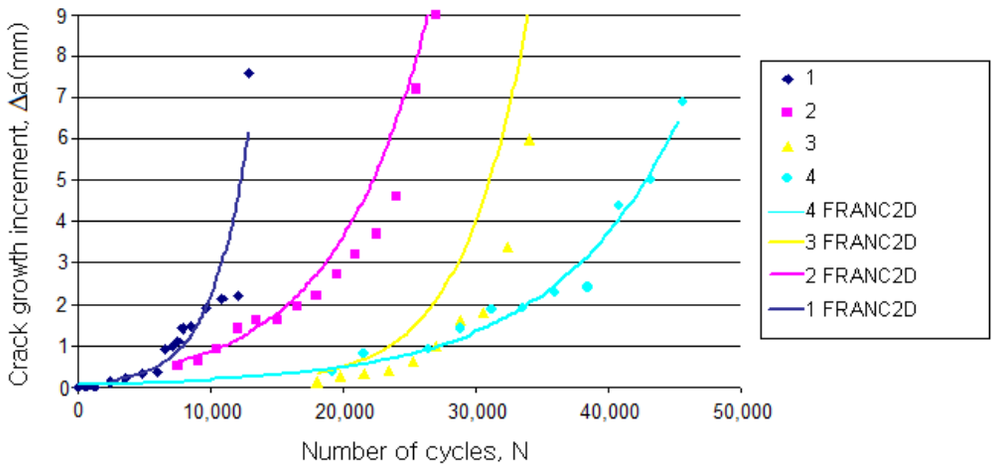

Figure 14. FRANC2D and experimental analysis results for M(T) specimens obtained from FGM2.

3. Conclusions

In the literature, studies related to FGM have mostly focused on determining FGMs' thermal properties using experimental, analytical, and numerical methods. FGMs' fatigue and fatigue fracture behaviors have been tested using numerical and analytical methods and improved new approaches are developed to date. However, there are hardly enough experimental studies to support this.

In conjunction with this study, mechanical properties and fatigue crack propagation behavior were analyzed experimentally. The results can be summarized as follows:

1. FGMs can be manufactured easily by centrifugal casting. It is possible to obtain FGM having different properties by changing casting parameters, FGM thickness, and casting weight from reinforced mixture.

2. Since SiC density is higher than aluminum, it is dispersed mostly to the outer region of material because of the centrifugal force during centrifugal casting. Therefore, hardness, composition, and mechanical properties change throughout the FGM thickness.

3. Crack propagation behaviors of single-edge notched (SE(T)) on SiC-rich side and single-edge notched (SE(T)) on aluminum-rich side specimens are different from each other under the same fatigue load. Fatigue crack propagation both begins later and has long fatigue life on SiC-rich side.

4. Each middle tension M(T) specimen obtained by slicing wall thickness as four sections shows different crack propagation behaviors. As SiC rate increases, crack begins and propagations are delayed under the same experimental conditions. After all, fatigue life increases to approximately 350%.

5. $p < 1$ seems to be more advantageous than $p > 1$ condition after crack propagation experiments of FGM when crack propagation starts from single-edge notched (SE(T)) aluminum-rich side considering the gradient exponent.

Acknowledgements

This study was supported by the Scientific Research Department of Pamukkale University as a PhD. Thesis via Project 2009FBE006 [88]. Some parts of this study were presented in the 16th International Conference on Machine Design and Production.

Author details

Arzum Ulukoy[1*], Muzaffer Topcu[2] and Suleyman Tasgetiren[3]

*Address all correspondence to: aulukoy@pau.edu.tr

1 Manufacturing Engineering Department, Faculty of Technology, Pamukkale University, Denizli, Turkey

2 Mechanical Engineering Department, Faculty of Engineering, Pamukkale University, Denizli, Turkey

3 Mechanical Engineering Department, Faculty of Engineering, Bursa Orhangazi University, Bursa, Turkey

References

[1] Ashby MF. Materials Selection in Mechanical Design. Burlington: Butterworth-Heinemann Linacre House, Jordan Hill, Oxford OX28DP30 Corporate Drive; 2004. pp. 80–81.

[2] Wojciechowski S. New trends in the development of mechanical engineering materials. J Mater Process Technol. 2000; 106(1): 230–235.

[3] Mukerji J. Ceramic matrix composites. Defence Sci J. 2013; 43(4): 385–395.

[4] Cirakoglu M. Processing and characterization of functionally graded titanium/titanium boride/titanium diboride composites by combustion synthesis/compaction and microwaves [thesis]. University of Idaho; 2001.

[5] Yamamoto G and Hashida T. Carbon nanotube reinforced alumina composite materials. In: Hu N, editor. Composites and Their Properties. p. 483. InTech, Rijeka, Cro-

atia, DOI: 10.5772/48667; 2012. Available from: www.intechopen.com/books/composites-and-their-properties/carbon-nanotube-reinforced-alumina-composite-materials.

[6] Ahmad Z and Aleem JA. Corrosion behavior of aluminium metal matrix composite. In: Ahmad Z, editor. Recent Trends in Processing and Degradation of Aluminium Alloys. p. 385. InTech, Rijeka, Croatia, DOI: 10.5772/23631; 2011. Available from: www.intechopen.com/books/recent-trends-in-processing-and-degradation-of-aluminium-alloys/corrosion-behavior-of-aluminium-metal-matrix-composite.

[7] Chawla N and Chawla KK. Metal Matrix Composites. New York: Springer Science + Business Media; 2006.

[8] Tilbrook MT, Moon RJ, and Hoffman M. Crack propagation in graded composite. Compos Sci Technol 2005;65: 201–220.

[9] Cho JR and Oden JT. Functionally graded material: a parametric study on thermal-stress characteristics using the crank-nicolson-galerkin scheme. Comput Meth Appl Mech Eng. 2000;188: 17–38.

[10] Reimanis IE. Functionally graded materials. In: Wessel JK, editor. Handbook of Advanced Materials: Enabling New Designs. Wiley-Interscience, Hoboken, New Jersey; 2004. pp. 465–487.

[11] Koizumi M. The concept of FGM. Ceram Trans Funct Gradient Mater. 1993; 34: 3–10.

[12] Rassbach S and Lehnert W. Investigations of deformation of FGM. Comp Mater Sci. 2000; 19: 298–303.

[13] Xu FM, Zhu SJ, Zhao J, Qi M, Wang FG, Li SX, and Wang ZG. Effect of stress ratio on fatigue crack propagation in a functionally graded metal matrix composite. Compos Sci Technol. 2004; 64: 1795–1803.

[14] Oyelayo AO and Haselkorn MH. Modified boron containing coating for improved wear and pitting resistance. U.S.A. Patent. 2002; patent number: 6432480.

[15] Cetinel H, Uyulgan B, Tekmen C, Ozdemir I, and Celik E.. Wear properties of functionally gradient layers on stainless steel substrates for high temperature applications. Surf Coat Technol. 2003; 174–175: 1089–1094.

[16] Demirkiran AS, Celik E, Yargan M, and Avcı E. Oxidation behaviour of functionally gradient coatings including different composition of cermets. Surf Coat Technol. 2001; 142–144: 551–556.

[17] Burris KW, Beardsley MB, and Chuzhoy L. Process for applying a functionally gradient coating to a component for improved performance. U.S.A. Patent. 2000; patent number: 6048586

[18] Ichikawa K Functionally Graded Materials in the 21st Century: A Workshop on Trends and Forecasts. Boston: Kluwer Academic Publishers; 2001.

[19] Biesheuvel MP and Verweij H. Calculation of the composition profile of a functionally graded material produced by centrifugal casting. J Am Ceram Soc. 2000; 83: 743–749.

[20] Qin XH, Han WX, Fan CG, Rong LJ, and Li YY. Research on distribution of SiC particles in aluminum-alloy matrix functionally graded composite tube manufactured by centrifugal casting. J Mater Sci Lett. 2002; 21: 665–667.

[21] Zhang J, Wang YQ, Zhou BL, and Wu XQ. Functionally graded Al/Mg2Si in-situ composites prepared by centrifugal casting. J Mater Sci Lett. 1998; 17: 1677–1679.

[22] Sivakumar R, Nishikawa T, Honda S, Awaj H, and Gnanam FD. Processing of mullite-molybdenum graded hollow cylinders by centrifugal molding technique. J Eur Ceram Soc. 2003; 23: 765–772.

[23] Watanabe Y, Yamanaka N, and Fukui Y. Control of composition gradient in a metal-ceramic functionally graded material manufactured by the centrifugal method. Compos Part A Appl Sci Manuf. 1998; 29: 595–601.

[24] Watanabe Y, Yamanaka N, and Fukui Y. Wear behavior of Al-Al3Ti composite manufactured by a centrifugal method. Metall Mater Trans A. 1999; 30(12): 3253–3261.

[25] Watanabe Y, Kawamoto A, and Matsuda K. Particle size distributions in functionally graded materials fabricated by the centrifugal solid-particle method. Compos Sci Technol. 2002; 62: 881–888.

[26] Lee NJ, Jang J, Park M, and Choe CR. Characterization of functionally gradient epoxy/carbon fibre composite prepared under centrifugal force. J Mater Sci. 1997; 32: 2013–2020.

[27] Kim JK and Rohatgi PK. Formation of a graphite-rich zone in centrifugally cast copper alloy graphite composites. J Mater Sci. 1998; 33: 2039–2045.

[28] Chen W, Wang Q, Zai C, Ma C, Zhu Y, and He W. Functionally graded Zn-Al-Si in-situ composites fabricated by centrifugal casting. J Mater Sci Lett. 2001; 20: 823–826.

[29] Duque NB, Melgarejo ZH, and Suarez OM. Functionally graded aluminum matrix composites produced by centrifugal casting. Mater Charact. 2005;55:167-171.

[30] Ahmad SNAS, Hashim J, and Ghazali MI. Effect of porosity on tensile properties of cast particle reinforced MMC. J Compos Mater. 2005; 39(5): 451–466.

[31] Kinemuchi Y, Wataria K, and Uchimurab K. Centrifugal sintering of ceramics. J Eur Ceram Soc. 2004; 24: 2061–2066.

[32] Gupta M. Functionally gradient materials and the manufacture thereof. U.S.A. Patent. 2002; patent number: 6495212

[33] Groza JR, and Kodash V. Methods for production of FGM net shaped body for various applications. U.S.A. Patent. 2006; patent number: 0172073.

[34] Paris PC and ErdoganA critical analysis of crack propagation lawsJ Basic Eng196385(4)528–533.

[35] Delale F and Erdogan F. The crack problem for a nonhomogeneous plane. J Appl Mech. 1983; 50: 609–614.

[36] Erdogan F. The crack problem for bonded nonhomogeneous materials under anti-plane shear loading. J Appl Mech. 1985; 52: 823–828.

[37] Erdogan F. Fracture mechanics of functionally graded materials. Compos Eng. 1995; 5(7): 753–770.

[38] Erdogan F. Fracture mechanics of functionally graded materials. U.S. Air Force Office of Scientific Research Final Technical Report. October 1996.

[39] Eischen JW. Fracture of nonhomogeneous materials. Int J Fract. 1987; 34: 3–22.

[40] Konda N and Erdogan F. The mixed mode crack problem in a nonhomogeneous elastic medium. Eng Fract Mech. 1994; 47(4): 533–545.

[41] Jin ZH and Noda N. Crack-tip singular fields in nonhomogeneous materials. J Appl Mech. 1994; 61: 738–740.

[42] Jin ZH and Batra RC. Some basic fracture mechanics concepts in functionally graded materials. J Mech Phys Solids. 1996; 44(8): 1221–12234.

[43] Gu P and Asaro RJ. Cracks in functionally graded materials. Int J Solids Struct. 1997; 34(1): 1–17.

[44] Lee YL and Erdogan F. Interface cracking of FGM coatings under steady-state heat flow. Eng Fract Mech. 1998;59(3):361-380.

[45] Xu FM, Zhu SJ, Zhao J, Qi M, Wang FG, Li SX and Wang ZG. Effect of stress ratio on fatigue crack propagation in a functionally graded metal matrix composite. Composites Science and Technology. 2004;64:1795-1803.

[46] Guler MA and Erdogan F. The frictional sliding formulations upon which subsequent analysis of the contact problems of rigid parabolic and cylindrical tangential loading problem will be performed in stamps on graded coatings. Int. J. Mech. Sci. 2007;49:161-182.

[47] Chen J, Wu L and Du S. A modified J integral for functionally graded materials. Mechanics Research Communications. 2000;27(3):301-306.

[48] Weichen S. On the dynamic energy release rate in functionally graded materials. International Journal of Fracture. 2005;131(3):31-35.

[49] Kolednik O. The yield stress gradient effect in inhomogeneous materials. Int J Solids Struct. 2000; 37: 781–808.

[50] Konda N and Erdogan F. The mixed mode crack problem in a nonhomogeneous elastic medium. Eng Fract Mech. 1994; 47(4): 533–545.

[51] Oral A, Çopur IH, and Anlas G. Özellikleri fonksiyonel olarak değişen malzemelerde karışık mod yükleme altında çatlak başlama açıları ve gerilim şiddet çarpanları. In: 8. Ulusal Kırılma Konferansı Bildiriler Kitabı; November 7–9 2007; Istanbul, Turkey; 2007. pp. 10–19.

[52] Yıldırım B, Dag S, and Erdogan F. Three dimensional fracture analysis of FGM coatings under thermomechanical loading. Int J Fract. 2005; 132: 369–395.

[53] Chung TJ, Neubrand A, Rödel J, and Fett T. Fracture toughness and r-curve behaviour of Al_2O_3/Al FGMs. Ceram Trans. 2001; 114: 789–796.

[54] Moon RJ, Hoffman M, Hilden J, Bowman KJ, Trumble KP, and Rödel. R-Curve behaviour in alumina-zirconia composites with repeating graded layers. J. Eng Fract Mech. 2002; 69: 1647–1665.

[55] Forth SC, Favrow LH, Keat WD, and Newman JA. Three-dimensional mixed-mode fatigue crack growth in a functionally graded titanium alloy. Eng Fract Mech. 2003; 70: 2175–2185.

[56] Xu FM, Zhu SJ, Zhao J, Qi M, Wang FG, Li SX, and Wang ZG. Fatigue crack growth in SiC particulate-reinforced Al matrix graded composite. Mater Sci Eng A. 2003; 360: 191–196.

[57] Xu FM, Zhu SJ, Zhao J, Qi M, Wang FG, Li SX, and Wang ZG. Comparison of the fatigue growth behaviour in homogeneous and graded SiC particulate reinforced Al composite. J Mater Sci Lett. 2003; 22: 899–901.

[58] Balke H, Bahr HA, Semenov AS, Hofinger I, Häusler C, Kirchhoff G, and Weiss HJ. Graded thermal barrier coatings: Cracking due to laser irradiation and determining of fracture toughness. Ceram Trans. 2001; 114: 205–212.

[59] Hofinger I, Bahr HA, Balke H, Kirchhoff G, Häusler C, and Weiß HJ. Fracture mechanical modelling and damage characterisation of functionally graded thermal barrier coatings by means of laser irradiation. Mater Sci Forum. 1999; 308(311): 450–456.

[60] Rousseau CE and Tippur HV. Compositionally graded materials with cracks normal to the elastic gradient. Acta mat. 2000; 48: 4021–4033.

[61] Hoffman M, Kidson L, Kelly D, and Deneke C. Effect of crack growth resistance upon fracture of ceramic/polymer graded interfaces. In: Ravi-Chandar K, Karihaloo BL, Kishi T, Ritchie RO, Yokobori AT, Yokobori T, editors. Advances in Fracture Research, Proc. ICF10; Pergamon2001.

[62] Chapa-Cabrera JG and Reimanis IE. Effects of residual stress and geometry on predicted crack paths in graded composites. Eng Fract Mech. 2002; 69: 1667–1678.

[63] Tilbrook MT. Fatigue crack propagation in functionally graded materials [thesis]. University of New South Wales; 2005.

[64] Lin JS and Miyamoto Y. Internal stress and fracture behaviour of symmetric Al2O3/TiC/Ni FGMs. Mater Sci Forum. 1999; 308(311): 855–860.

[65] Freund LB. Stress distribution and curvature of a general compositionally graded semiconductor layer. J Crystal Growth. 1993; 132(1–2): 341–344.

[66] Shabana YM and Noda N. Thermo-elastic-plastic stresses in functionally graded materials subjected to thermal loading taking residual stresses of the fabrication process into consideration. Composites: B. 2001; 32: 111–121.

[67] Anderson TL. Fracture Mechanics: Fundamentals & Applications. Boca Raton: CRC Press; 1995.

[68] Parameswaran V and Shukla A. Crack-tip stress fields for dynamic fracture in functionally graded materials. Mech Mater. 1999; 31: 579–596.

[69] Chen YF and Erdogan F. The interface crack problem for a nonhomogeneous coating bonded to a homogeneous substrate. J Mech Phys Solids. 1996; 44: 771–787.

[70] Bao G and Wang L. Multiple cracking in functionally graded ceramic/metal coatings. Int J Solids Struct. 1995; 32(19): 2853–2871.

[71] Bleek O, Munz D, Schaller W, and Yang YY. Effect of a graded interlayer on the stress intensity factor of cracks in a joint under thermal loading. Eng Fract Mech. 1998; 60(5–6): 615–623.

[72] Wang YS and Gross D. Analysis of a crack in a functionally gradient interface layer under static and dynamic loading. Key Eng Mater. 2000; 187(183): 331–336.

[73] Chung TJ, Neubrand A, and Rödel J. Effect of residual stress on the fracture toughness of Al_2O_3/Al gradient materials. Key Eng Mater. 2002; 206(213): 965–968.

[74] Duque NB, Melgarejo ZH, and Suarez OM. Functionally graded aluminum matrix composites produced by centrifugal casting. Mater Charact. 2005; 55: 167–171.

[75] Quadrini E. Microstructural characterization of a silicon carbide whisker reinforced 2014 aluminum metal matrix composite. Journal De Physique, IV Colloque C7, SupplBment au Journal de Physique. 1993; 111(3): 1741–1744.

[76] Melgarejo ZH, Sua´ rez OM, and Sridharan K. Wear resistance of a functionally-graded aluminum matrix composite. Scr Mater. 2005; 55: 95–98.

[77] Rajan TPD, Pillai RM, and Pai BC. Characterization of centrifugal cast functionally graded aluminum-silicon carbide metal matrix composites. Mater Charact. 2010; 61: 923–928.

[78] Vieira AC, Sequeira PD, Gomes JR, and Rocha LA. Dry sliding wear of Al alloy/SiC functionally graded composites: Influence of processing conditions. Wear. 2009; 267: 585–592.

[79] Watanabe Y and Nakamura T. Microstructures and wear resistances of hybrid Al-(Al3TişAl3Ni) FGMs fabricated by a centrifugal method. Intermetallics. 2001; 9: 33–43.

[80] Kai W, Xue HS, Zou MH, Liu CM. Microstructural characteristics and properties in centrifugal casting of SiCp/Zl104 composite. Trans Nonferrous Met Soc China. 2009; 19: 1410–1415.

[81] Tokaji K. Effect of stress ratio on fatigue behaviour in SiC particulate-reinforced aluminium alloy composite. Fatigue Fract Eng Mater Struct. 2005; 28: 539–545.

[82] Ulukoy A, Topcu M, and Tasgetiren S. The effect of aging treatments on wear behavior of aluminum matrix functionally graded material under wet and dry sliding conditions. Mat wiss u Werkstofftech. 2011; 42: 806–811.

[83] Ulukoy A, Topcu M, and Tasgetiren S. Experimental investigation of aluminum matrix functionally graded material: Microstructural and hardness analyses, fretting, fatigue, and mechanical properties.. Proceedings of the Institution of Mechanical Engineers, Part J: Journal of Engineering Tribology. DOI: 10.1177/1350650115594405

[84] Uluköy A, Topçu M, and Taşgetiren S. Experimental investigation of crack propagation in aluminum matrix functionally graded material. In: UMTIK-2014 16th International Conference on Machine Design and Production; June 30–July 3, Izmir, Turkey, 2014.

[85] ASTM E647. Standard Test Method for Measurement of Fatigue Crack Growth Rates. ASTM International, 100 Barr Harbor Drive, PO Box C700, West Conshohocken, PA 19428-2959; 2011.

[86] Ergun E. Fracture and fatigue analysis of repaired cracks in aluminum plates with composite patch under temperature and moisture [thesis]. Pamukkale University; 2009.

[87] www.cfg.cornell.edu/software.html, Cornell Fracture Group, 02/04/2016 [Internet].

[88] Ulukoy A. Experimental and numerical analysis of fretting fatigue behavior of functionally graded material manufactured by centrifugal casting [thesis]. Pamukkale University; 2011.

IntechOpen